ELSEVIER

Journal of Molecular Catalysis A: Chemical 108 (1996) 167–174

JOURNAL OF MOLECULAR CATALYSIS A: CHEMICAL

Raman spectroscopy studies on the structure of MoO_3/ZrO_2 solid superacid

Biying Zhao *, Xiaoyong Wang, Huarong Ma, Youqi Tang

Institute of Physical Chemistry, Peking University, Beijing 100871, China

Received 15 August 1995; accepted 19 December 1995

Abstract

MoO_3/ZrO_2 prepared by different methods are distinctive in catalytic behavior. MoO_3/ZrO_2 (MZ) obtained by impregnating crystallized ZrO_2 and then calcining at high temperature is a catalyst for partial oxidation. However, MoO_3/ZrO_2 (MZH) obtained by impregnating $Zr(OH)_4$ and then calcining at high temperature is a solid superacid. It has been proved by Raman spectroscopy that they have different structural characteristics. In the MZ sample MoO_3 is present as a monolayer, i.e., two-dimensional polymolybdates on monoclinic ZrO_2, whose characteristic broad band is at about 950 cm^{-1}. As MoO_3 content is beyond its monolayer dispersion capacity (0.12 g $MoO_3/100$ m^2 ZrO_2), the surplus MoO_3 is present as crystalline MoO_3, whose intense peaks are at 820 and 994 cm^{-1}. As for MZH sample, MoO_3 exists on metastable tetragonal ZrO_2 ($ZrO_2(t)$) in two kinds of surface states, i.e., two-dimensional polymolybdates and Mo–O–Zr surface species which have a broad band at about 814 cm^{-1}. Mo(VI) in Mo–O–Zr surface species is tetra-coordinated and bonds strongly with $ZrO_2(t)$. As MoO_3 content in MZH sample exceeds a certain value, bulk $Zr(MoO_4)_2$ appears, which is indicated by the appearance of sharp peaks at 750, 946, 326 and 1002 cm^{-1}. Quantitative Raman measurements for the three states of MoO_3 in MZH samples show that the Mo–O–Zr surface species may be a preliminary compound of bulk $Zr(MoO_4)_2$. There is a good corresponding relation between its content and the catalytic activity of the superacid, therefore it should be responsible for its superacidity.

Keywords: Superacid; Molybdenum(VI) oxide; Zirconia; Raman spectra; Quantitative Raman analysis; Surface states

1. Introduction

Any acid can be termed a superacid if its acidity is stronger than that of 100% H_2SO_4, i.e. $Ho \leq -12.0$ [1]. The catalytic activity of superacids for many reactions of hydrocarbon transformations is surprisingly high. They can even activate methane at low temperature [2,3].

As catalysts, solid acids have some additional advantages, such as ease of separation from a reaction mixture, no corrosion for the reactor, and free from pollution, etc. So they are worthy of attention in theoretical research and in synthetic application [3,4].

In 1988, Arata and Hino [5–8] reported that solid superacid could be synthesized by supporting WO_3 or MoO_3 on ZrO_2 or TiO_2 under certain preparation conditions. These superacids can remain stable even at high temperature and in a solid–liquid system, so they have better application prospects than other solid su-

* Corresponding author. E-mail: zhaoby@pschnetware.pku.edu.cn

PII S1381-1169(96)00008-8

peracids, as SbF_5 or sulfate supported on metal oxides do.

Research on the MoO_3/ZrO_2 system showed that MoO_3/ZrO_2 prepared by impregnating $Zr(OH)_4$ with the solution of ammonium heptamolybdate and then drying and calcining at 700–800°C is a solid superacid [5–8], while MoO_3/ZrO_2 prepared by impregnating crystallized ZrO_2 and then drying and calcining is only a catalyst for partial oxidation [9,10]. It was reported [5–8] that ZrO_2 is tetragonal in the former and monoclinic in the latter. In addition, the specific surface area of the former is greater than that of the latter. In order to elucidate the surface properties of MoO_3/ZrO_2 catalysts, XPS measurement was used, and it was found that the binding energies of Mo $3d_{3/2}$, Zr $3d_{5/2}$ and O 1s in both catalysts were quite similar to those of pure MoO_3 and ZrO_2 [5–8].

However, the following questions are still open: Why the preparation methods gave such a decisive effect on their catalytic behavior? What are the differences between the structures of these two kinds of MoO_3/ZrO_2 catalysts? What should be responsible for the superacidity of MoO_3/ZrO_2 system?

Since Raman spectroscopy can provide detailed information about the active phases of MoO_3-supported catalysts [11], we have chosen the MoO_3/ZrO_2 system as the object of our research although its acidity is not the strongest among the known solid superacids. By Raman spectroscopy, we have found that there are many obvious differences between the structures of the MoO_3/ZrO_2 catalysts prepared by the two different methods, and there is a specific surface state of molybdenum in the MoO_3/ZrO_2 solid superacid, which is closely related to its superacidity.

2. Experimental

2.1. Sample preparation

$Zr(OH)_4$ was obtained by adding 3.3 M ammonia solution to 1 M $ZrOCl_2$ solution till pH 10. The precipitate was washed with water until the filtrate showed a negative test for Cl^-, and then dried at 110°C. ZrO_2 was obtained by calcining $Zr(OH)_4$ at 550°C. MZH and MZ samples were prepared by impregnating $Zr(OH)_4$ and ZrO_2 with a series of ammonium heptamolybdate solutions respectively, followed by drying and calcining at suitable temperatures.

2.2. Raman spectroscopy measurement

Raman spectra was recorded by using a Ramanor U-1000 double monochromater with 1800 gr/mm holographic gratings. A Spectra Physics Model Stabilite-2016 argon laser was used to supply 514.5 nm exciting line. The laser power was adjusted to about 100 mW. The slit width was 1 cm^{-1}, and the wavenumbers obtained from the spectra were accurate within 2 cm^{-1}. The powdered samples were pressed into wafers and rotated at high speed to avoid any damage due to laser-induced heat effects.

In quantitative Raman determination, KNO_3 was chosen as an internal standard [12,13] and added to each sample in adequate weight percentages. The areas of some characteristic peaks of the active component (I_a's) and the peak area of KNO_3 at 1050 cm^{-1} (I_{KNO_3}) were measured, then normalized into the peak area ratios (I_a/I_{KNO_3}) when there are equal amounts of KNO_3 and ZrO_2 in the samples. The normalized ratios were regarded as the relative contents of relevant phases of the active component.

2.3. XRD and XPS measurement

The identification of phases was carried out by means of a BD-86 X-ray diffractometer, employing CuK_α (Ni-filtered) radiation.

XPS data were measured on a VG-ESCA LAB5 electron spectrometer, using AlK_α radiation (10 kV, 40 mA). The spectra were obtained at room temperature and 10^{-8} Torr. The XPS intensity ratio of Mo $3d_{3/2}$ to Zr $3d_{5/2}$ (I_{Mo}/I_{Zr}) was calculated from relative peak area ratio of

Mo $3d_{3/2}$ level to Zr $3d_{5/2}$ level, and was taken as the measurement of their surface concentration on the sample [14].

3. Results and discussion

It has been found by Raman spectroscopy that there are many obvious differences between the structures of MZH and MZ samples.

3.1. Morphology of the support ZrO_2

Zirconia as support of catalysts involves two phases: stable monoclinic zirconia ZrO_2(m) and metastable tetragonal zirconia ZrO_2(t), which can be revealed by their different Raman spectra [15]. The ZrO_2 obtained by calcining pure $Zr(OH)_4$ at 550°C for 4 h is mostly monoclinic. Therefore, the ZrO_2 in MZ samples obtained by impregnating this kind of crystallized ZrO_2 is also monoclinic (See Fig. 1).

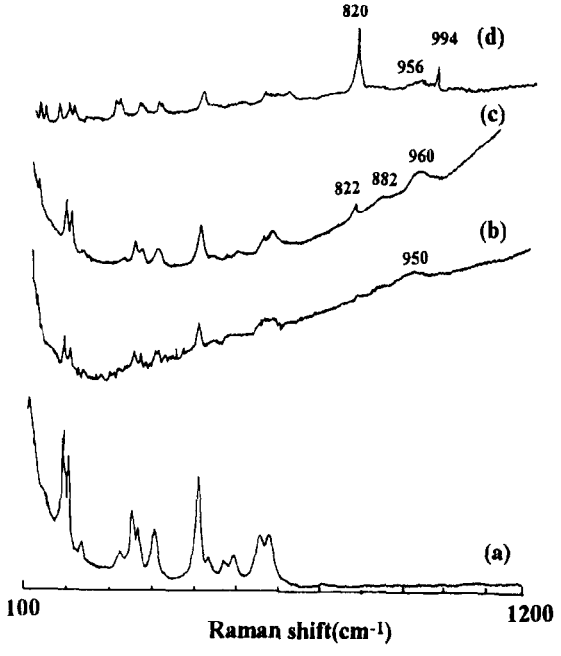

Fig. 1. Raman spectra of ZrO_2 and some MZ samples calcined at 550°C for 4 h. (a) ZrO_2; (b) 0.04 g MoO_3 /g ZrO_2; (c) 0.08 g MoO_3 /g ZrO_2; (d) 0.13 g MoO_3 /g ZrO_2.

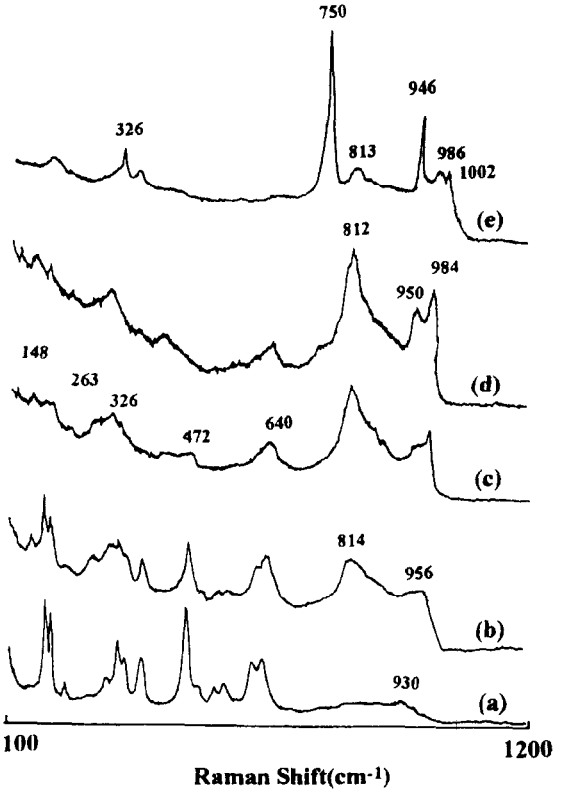

Fig. 2. Raman spectra of MZH samples calcined at 550°C for 4 h. (a) 0.03 g MoO_3 /g ZrO_2; (b) 0.09 g MoO_3 /g ZrO_2; (c) 0.16 g MoO_3 /g ZrO_2; (d) 0.26 g MoO_3 /g ZrO_2; (e) 0.42 g MoO_3 /g ZrO_2.

However, there is a different situation for MZH samples (see Fig. 2):

(1) For MZH samples calcined at 550°C, the larger the content of MoO_3, the greater the proportion of ZrO_2(t) that has characteristic broad peaks at 148, 263, 326, 472 and 640 cm^{-1}. As the MoO_3 content reaches a certain level, nearly all the ZrO_2 in the MZH sample is tetragonal.

(2) After calcination at 600°C or even 750°C, the tetragonal ZrO_2 is still dominant as long as the MoO_3 content is high enough (see Figs. 3 and 4). This result is also supported by their XRD results (see Fig. 5).

It was reported that ZrO_2 will exist in a metastable tetragonal phase rather than a stable monoclinic phase as its crystallite size is smaller than the critical value [16]. Therefore, it can be

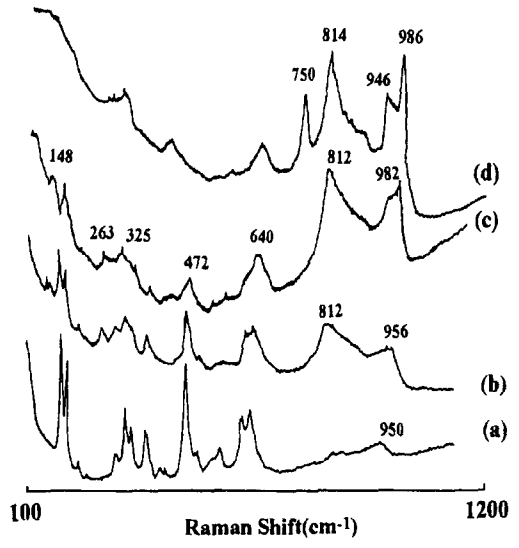

Fig. 3. Raman spectra of MZH samples calcined at 600°C for 4 h. (a) 0.03 g MoO_3 /g ZrO_2; (b) 0.09 g MoO_3 /g ZrO_2; (c) 0.16 g MoO_3 /g ZrO_2; (d) 0.26 g MoO_3 /g ZrO_2.

expected that the crystalline size of ZrO_2 in MZH should be smaller, and its specific surface area should be greater as a result. This point has been proved by the experiment results [17]. For example, as the MoO_3 content is about 0.28 g MoO_3/g ZrO_2 and the calcination temperature is 550°C, the surface area of the MZH sample is about 200 m^2/g, whereas that of the MZ sample is only about 30 m^2/g.

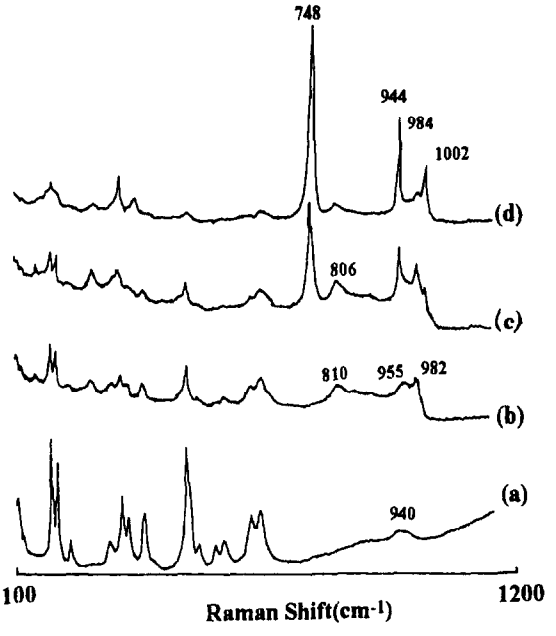

Fig. 4. Raman spectra of MZH samples calcined at 750°C for 4 h. (a) 0.03 g MoO_3 /g ZrO_2; (b) 0.09 g MoO_3 /g ZrO_2; (c) 0.16 g MoO_3 /g ZrO_2; (d) 0.26 g MoO_3 /g ZrO_2.

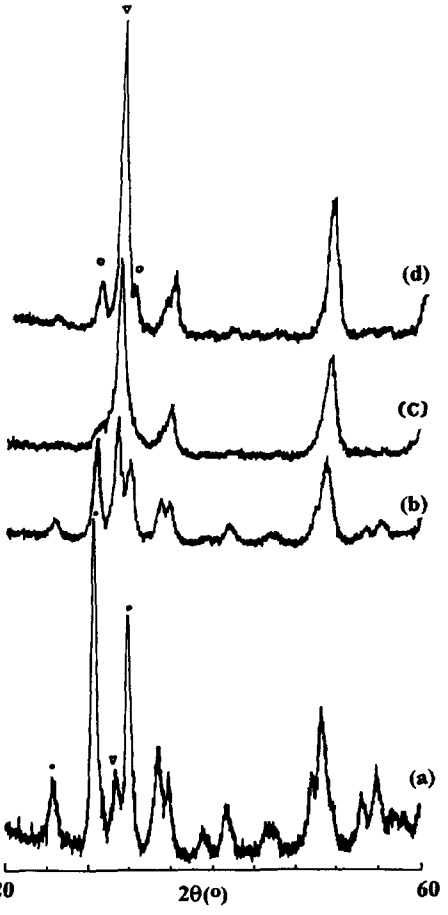

Fig. 5. XRD results of ZrO_2 and MZH samples. (▽, tetragonal ZrO_2; O, monoclinic ZrO_2.) (a) ZrO_2, 550°C; (b) MZH, 0.03 g MoO_3 /g ZrO_2 550°C; (c)MZH, 0.09 g MoO_3 /g ZrO_2 550°C; (d) MZH, 0.09 g MoO_3 /g ZrO_2 750°C.

3.2. Morphology of the active component MoO_3

3.2.1. MZ samples

From Fig. 1 it can be seen that MoO_3 in MZ samples is dispersed on the surface of zirconia as a monolayer state, i.e. two-dimensional polymolybdates, which gives rise to the characteristic broad band at about 960 cm^{-1} [18–20]. As

MoO_3 loading exceeds a certain value, the surplus MoO_3 is present as crystalline form. In this case, the sharp peaks at 820 and 994 cm^{-1} due to the crystalline MoO_3 can be observed.

The quantitative Raman measurement has been carried out for MZ samples calcined at 550°C. The peak at 820 cm^{-1} of crystalline MoO_3 and the peak at 1050 cm^{-1} of KNO_3 were measured and the Raman intensity ratios I_{820}/I_{1050} was obtained. The contents of crystalline MoO_3 in the samples have been derived by referring to the calibration curves for MoO_3–KNO_3 mixtures. Fig. 6 shows the content of crystalline MoO_3 as a function of the total content of MoO_3 in the MZ samples, from which the MoO_3 utmost dispersion capacity on ZrO_2, 0.065 g MoO_3/g ZrO_2 is deduced. Since the surface area of ZrO_2 used as support is 54 m^2/g, this capacity is equivalent to 0.12 g MoO_3/100 m^2 ZrO_2, which is consistent with its theoretical monolayer capacity [20–22].

The XPS results show that the binding energies of Mo $3d_{3/2}$, Zr $3d_{5/2}$ and O 1s in both MZ and MZH samples are similar to those of pure MoO_3 and ZrO_2 respectively, which confirms the results reported by Hino and Arata [5]. The curves in Fig. 7 represent the XPS peak intensity ratios of I_{Mo3d}/I_{Zr3d} as a function of total MoO_3 content. Since there are enormous differences in surface areas between MZ and MZH samples, we take g MoO_3/100 m^2 ZrO_2 for unit of total MoO_3 content. For MZ samples, the turning point in curve a is at 0.12 g MoO_3/100 m^2 ZrO_2, which is in good agreement with the MoO_3 utmost dispersion capacity deduced from the quantitative Raman measurement.

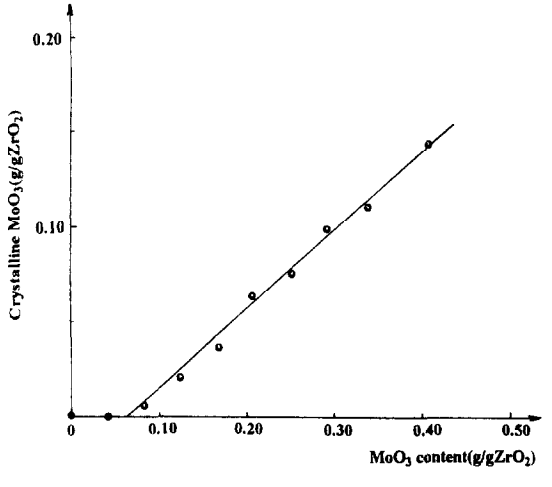

Fig. 6. Quantitative Raman spectra results of MZ samples.

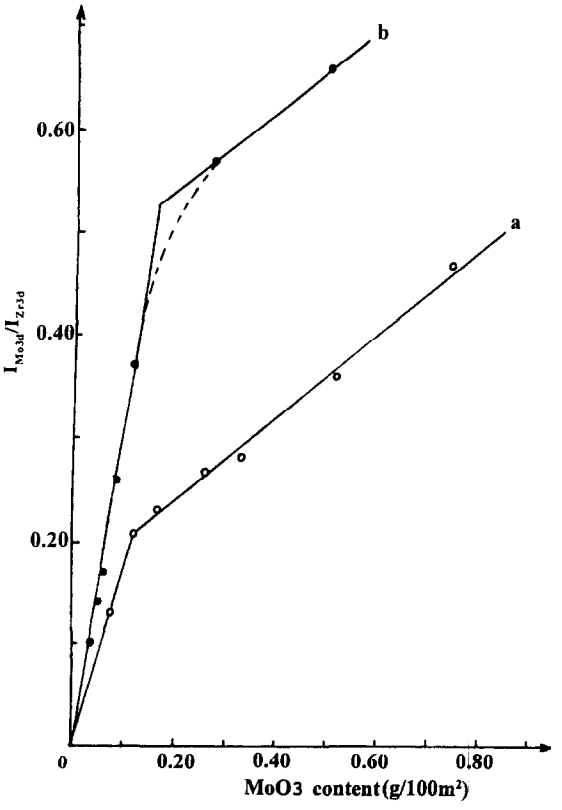

Fig. 7. Quantitative XPS results of the samples calcined at 550°C for 4 h. (a) MZ samples; (b) MZH samples.

3.2.2. MZH samples

The states of MoO_3 in MZH samples are quite different. It can be seen that an additional broad band at about 814 cm^{-1} appears besides the broad band at about 960 cm^{-1} in their Raman spectra (Fig. 2). As MoO_3 content gets beyond a certain value, a group of sharp peaks at 750, 946, 326, 1002 cm^{-1} due to the bulk $Zr(MoO_4)_2$ [23,24] is observed, which means

that the surplus MoO_3 has reacted with ZrO_2(t) and turned into bulk $Zr(MoO_4)_2$. Figs. 3 and 4 show that the situations of MZH samples calcined at 600°C and 750°C are similar.

We hold that the appearance of the broad band at about 814 cm^{-1} implies the formation of a new surface state in MZH samples. The reason is that the frequency of Mo=O stretching vibration in isolated tetra-coordination [MoO_4^{2-}] is 896 cm^{-1} [11], and when it combines strongly with ZrO_2 and forms

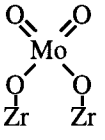

the vibration frequency of Mo=O terminal stretching would decrease. In addition, the serious broadening of the band shows that it may represent a surface state and its structure is heterogeneous. In the following, we will call it 'Mo–O–Zr surface species'. By comparing Fig. 2, Figs. 3 and 4, it can be seen that the higher the calcination temperature, the narrower the band at about 814 cm^{-1}, and the lower the frequency of this band. It means that as the calcination temperature rises, the combination between MoO_3 and ZrO_2 strengthens, and its structure becomes homogeneous. Since the acidity of MZH sample calcined at 700–800°C is the strongest, the frequency of Mo=O terminal stretching in Mo–O–Zr surface species, which shows the strength of the combination between MoO_3 and ZrO_2, is also relevant.

From the XPS results of MZH samples, we can see that: (i) The I_{Mo}/I_{Zr}'s of MZH samples are higher than those of MZ samples with the same total MoO_3 content. (ii) The turning point in curve b (Fig. 7) is 0.16 g MoO_3/100 m^2 ZrO_2, which is higher than the theoretical monolayer capacity of MoO_3 on ZrO_2.

These results also indicate that the surface structures of MZH samples are more complicated than those of the MZ samples. Moreover, it can be imagined that Mo in MZH sample should give a stronger XPS signal since there is bulk $Zr(MoO_4)_2$ under 'two-dimensional polymolybdate' or 'Mo–O–Zr surface species'.

3.3. Quantitative Raman spectroscopy results of MZH samples and the relationship between Mo–O–Zr surface species and its superacidity

In order to find out the relationship among the three states of MoO_3 in MZH sample, the relative areas of the two bands (at about 950 cm^{-1}, and at about 814 cm^{-1}) and the peak at 750 cm^{-1} to the peak at 1050 cm^{-1} of KNO_3 as an internal standard have been determined, and taken as the relative contents of two-dimensional polymolybdates, Mo–O–Zr surface

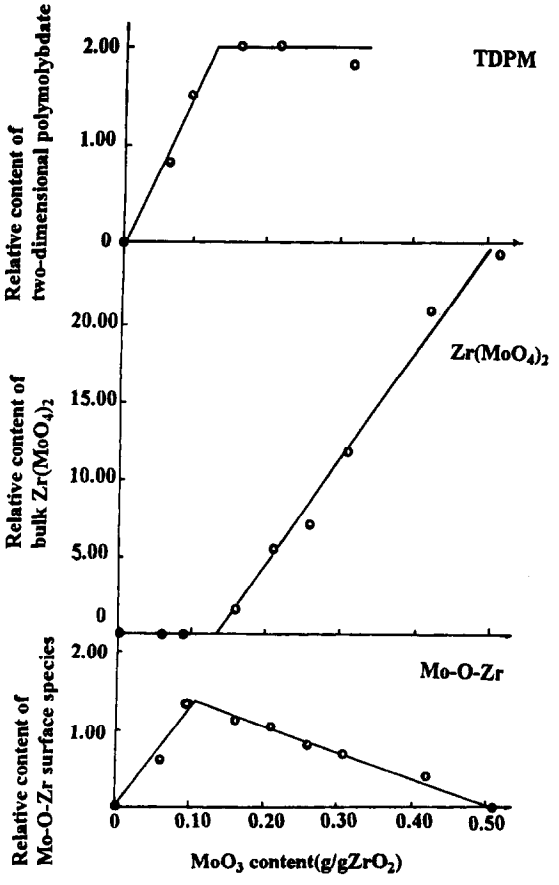

Fig. 8. Quantitative Raman spectra results of MZH samples calcined at 750°C. TDPM: two-dimensional polymolybdates.

species and bulk $Zr(MoO_4)_2$, respectively. The following are the results for MZH samples calcined at 750°C (See Fig. 8):

(1) The content of the two-dimensional polymolybdates increases with the total MoO_3 content of the sample, then remains the same once the MoO_3 content reaches a certain level.

(2) With increase of total MoO_3 content, the content of the Mo–O–Zr surface species increases and reaches a maximum, then gradually decreases to zero.

(3) The bulk $Zr(MoO_4)_2$ appears once the content of MoO_3 exceeds a certain value, after which its content rises linearly with increase in MoO_3 content.

The following two points are noticed from Fig. 8: (a) The turning points of the three curves are under the same total MoO_3 content. (b) The content of Mo–O–Zr surface species begins to decrease when the bulk $Zr(MoO_4)_2$ appears. Therefore, we consider that the Mo–O–Zr surface species may be the preliminary compound of bulk $Zr(MoO_4)_2$.

From the above results, it is not difficult to imagine that the Mo–O–Zr surface species that exists only in the MZH sample might be responsible for its superacidity. To prove this point, we have examined the activities of MZH sample at 200°C for cumene cracking which can be catalyzed at this temperature only by superacid [25].

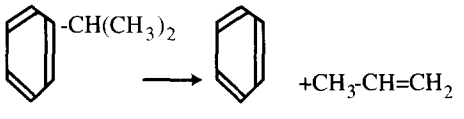

Fig. 9 shows a good corresponding relation between the conversion of cumene and the relative content of Mo–O–Zr surface species in MZH samples calcined at 750°C. These results are as expected. There are still some questions worthy of further study: Is this finding of general significance or not? Are there some relevant preliminary compounds responsible for the superacidity in WO_3/ZrO_2 and SO_4^{2-}/ZrO_2

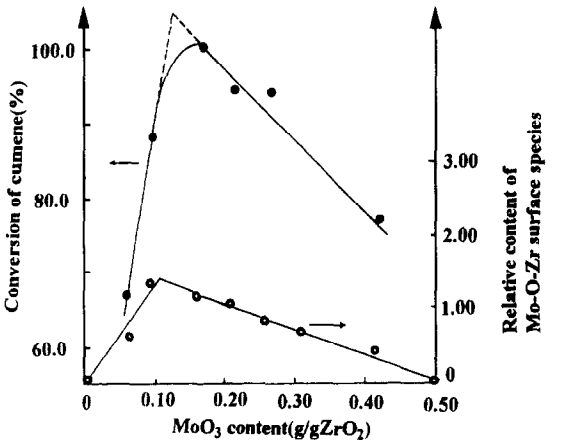

Fig. 9. The content of Mo–O–Zr surface species and the superacidity of MZH samples calcined at 750°C. (Reaction temperature: 200°C, 0.2 g catalyst.).

and so on? However, it is difficult to find effective characterization techniques for each superacid, just as Raman spectroscopy for MoO_3/ZrO_2 superacid.

4. Conclusions

Much new information on the structure of MoO_3/ZrO_2 catalysts has been obtained by using Raman spectroscopy, which can be summarized as follows:

(1) The tremendous differences in the catalytic behavior of MoO_3/ZrO_2 prepared by impregnating $Zr(OH)_4$ and crystalline ZrO_2 originate from their different structures, including the morphology of the support ZrO_2 and the active component MoO_3.

(2) In the MoO_3/ZrO_2 solid superacid, zirconia exists as metastable tetragonal modification, which has a large specific surface area and easily combines with MoO_3 to form Mo–O–Zr surface species. As the MoO_3 loading exceeds a certain level, Mo–O–Zr surface species develops into bulk $Zr(MoO_4)_2$.

(3) Mo–O–Zr surface species that exists only in MoO_3/ZrO_2 solid superacid should be responsible for its superacidity.

Acknowledgements

The support of the National Science Foundation of China and National Science and Technique Committee is gratefully acknowledged. With many thanks to Dr. Yinyan Huang, Mr. Yu Zhou, Mr. Xianping Xu, Ms. Xiaomin Pan and Mr. Qiang Fu for their help in the experiments and preparation of the manuscript.

References

[1] R.J. Gillespie and T.E. Peel, Adv. Phys. Org. Chem., 9 (1972) 1.
[2] G.A. Olah, G.K.S. Prakash and J. Sommer, Science, 13 (1979) 206.
[3] G.A. Olah, G.K.S. Prakash and J. Sommer, Superacids, Wiley, New York (1985).
[4] K. Tanabe, Solid Acids and Bases, Their Catalytic Properties, Tokyo Kodansha, Academic Press, New York, 1970.
[5] M. Hino and K. Arata, J. Chem. Soc. Chem. Commun., (1988) 1259.
[6] K. Arata and M. Hino, Chem. Lett., (1989) 971.
[7] K. Arata, Adv. catal., 37 (1990) 165.
[8] K. Arata and M. Hino, Mater. Chem. Phys., 26 (1990) 213.
[9] T. Ono, H. Miyata and Y. Kubokawa, J. Chem. Soc., Faraday Trans. I, 83 (1987) 1761.
[10] H. Miyata., S. Tokuda and T. Ono, J. Chem. Soc., Faraday Trans. I, 86 (1990) 2291.
[11] M.J. Stencel, Raman Spectroscopy for Catalysis, van Nostrand Reinhold, New York, 1989.
[12] J.P. Baltrus, L.E. Makovsky, J.M. Stencel and D.M. Hercules, Anal. Chem., 57 (1985) 2500.
[13] B.Y. Zhao, Q. Xu, Y.C. Xie and X.C. Yang, Chem. J. Chin. Univ. (China), 11 (1990) 54.
[14] L.L. Gui, Y.J. Liu, Q.L. Guo, H.Z. Huang and Y.Q. Tang, Sci. Sin. B, 28 (1985) 1233.
[15] P.D.L. Mereera, J.G. van Ommen, E.B.M. Doesberg, A.J. Burggranf and J.R.H. Ross, Appl. Catal., 57 (1990) 127.
[16] R.C. Garvie and M.F. Goss, J. Mater. Sci., 21 (1986) 1253.
[17] B.Y. Zhao, H.R. Ma and Y.Q. Tang, J. Catal. (China), 16 (1995) 177.
[18] R.B. Quincy, M. Houalla and D.M. Hercules, J. Catal., 106 (1987) 85.
[19] H. Jezlorowski, H. Knözinger, J. Phys. Chem., 83 (1974) 1166.
[20] Y.C. Xie, L.L. Gui, Y.J. Lin, B.Y. Zhao, N.F. Yang, Y.F. Zhang, Q.L. Guo, L.Y. Duao and Y.Q. Tang, Proc. Int. Congr. Catal., 8th, Vol. 5, 1984, p. 147.
[21] Y.C. Xie and Y.Q. Tang, Adv. Catal., 37 (1991) 1.
[22] B.Y. Zhao, Q. Xu, Y.C. Xie and X.C. Yang, Chem. J. Chin. Univ. (China), 11 (1990) 54.
[23] Y.L. Fu, W.J. Lu and J. Yang, J. Mol. Catal. (China), 5 (1991) 59.
[24] H.R. Ma, B.Y. Zhao, X.H. Cai, Y. Zhou and Y.Q. Tang, Petrochem. Technol. (Beijing), 24 (1995) 4.
[25] K. Arata, M. Hino and N. Yamagata, Bull. Chem. Soc. Jpn., 63 (1990) 244.